Performance Analysis of Wireless Network Aided by Discrete-Phase-Shifter IRS

Rongen Dong, Yin Teng, Zhongwen Sun, Jun Zou, Mengxing Huang, Jun Li, Feng Shu, and Jiangzhou Wang

***Abstract*—Discrete phase shifter of intelligent reflecting surface (IRS) generates phase quantization error (QE) and degrades the receive performance at the receiver. To make an analysis of the performance loss (PL) caused by IRS with phase QE, based on the law of large numbers, the closed-form expressions of signal-to-noise ratio (SNR) PL, achievable rate (AR), and bit error rate (BER) are successively derived under line-of-sight (LoS) channels and Rayleigh channels. Moreover, based on the Taylor series expansion, the approximate simple closed form of PL of IRS with approximate QE is also given. The simulation results show that the performance losses of SNR and AR decrease as the number of quantization bits increases, while they gradually increase with the number of IRS phase shifter elements increases. Regardless of LoS channels or Rayleigh channels, when the number of quantization bits is larger than or equal to 3, the performance losses of SNR and AR are less than 0.23 dB and 0.08 bits/s/Hz, respectively, and the BER performance degradation is trivial. In particular, the performance loss difference between IRS with QE and IRS with approximate QE is negligible when the number of quantization bits is not less than 2.**

***Index Terms*—Intelligent reflecting surface, performance loss, quantization error, Taylor series, the law of large numbers**

I. Introduction

With the rapid development of wireless networks, the demands for high rate, high quality, and ubiquitous wireless services will result in high energy consumption like the fifth generation (5G) systems [1]. To achieve an innovative, energy-efficient and low-cost wireless network, intelligent reflecting surface (IRS) has emerged as a new and promising solution. IRS, consisting of a large number of low-cost passive reflective elements integrated on a plane, can significantly enhance the performance of wireless communication networks by intelligently reconfiguring the wireless propagation environment [2]–[4]. There are heavy research activities on the investigation of various IRS-aided wireless networks [5]–[15].

Assuming that the line-of-sight (LoS) channels are employed, the authors in [16] maximized the secrecy rate (SR) by jointly optimizing IRS phases, and the trajectory and power control of unmanned aerial vehicle (UAV), based on the successive convex approximation, and the SR was significantly improved with the assistance of IRS. In [17], the authors discussed the characteristics of the UAV and IRS, and two cases were investigated by combining UAV and IRS to enhance the network throughput and security. In [18], a secure IRS-aided directional modulation network was investigated, and two alternating iterative algorithms, general alternating iterative and null-space projection, were proposed to maximize the SR. An IRS-assisted downlink multi-user multi-antenna system in the absence of direct links between the base station (BS) and user was proposed in [19], a hybrid beamforming scheme with continuous digital beamforming for the BS and discrete analog beamforming for the IRS was proposed to maximize sum-rate. In [20], the phase shifters of multiple IRSs were optimized to maximize rate, based on the least-squares method, the substantial rate gains were achieved compared to the baseline schemes. The problem of joint active and passive beamforming optimization for an IRS-aided downlink multi-user multiple-input multiple-output (MIMO) system was investigated in [21], where a vector approximate message passing algorithm was proposed to optimize the IRS phase shifts. In [22], the transmit covariance matrix and passive beamforming matrices of the two cooperative IRSs were jointly optimized to maximize rate, and a novel low-complexity alternating optimization algorithm was presented.

Actually, there are many works focusing on the beamforming methods and converge analysis in the Rayleigh channels. An IRS-assisted multiple-input single-output (MISO) system without eavesdropper's channel state information (CSI) was proposed in [23], in order to enhance the security, the oblique manifold method and minorization-maximization algorithms were proposed to jointly optimize the precoder and IRS phase shift. In [24], the continuous transmit beamforming at the access point (AP) and discrete reflect beamforming at the IRS were jointly optimized to minimize the transmit power at AP. An efficient alternating optimization algorithm was proposed and near-optimal performance was achieved. An IRS-aided secure multigroup multicast MISO communication system was proposed in [25], and the semidefinite relaxation scheme and a low-complexity algorithm based on second-order

Manuscript received April 13, 2022; revised June 13, 2022; approved for publication by Yajun Zhao, Guest Editor, Jul. 7, 2022.

This work was supported in part by the National Natural Science Foundation of China (Nos. 62071234, 62071289, and 61972093), the Hainan Province Science and Technology Special Fund (ZDKJ2021022), the Scientific Research Fund Project of Hainan University under Grant KYQD(ZR)-21008, and the National Key R&D Program of China under Grant 2018YFB180110.

R. Dong, Z. Sun, and M. Huang are with the School of Information and Communication Engineering, Hainan University, Haikou, 570228, China, email: dre2000@163.com, yukisoranya@gmail.com.

Y. Teng, J. Zou, and J. Li are with the School of Electronic and Optical Engineering, Nanjing University of Science and Technology, 210094, China, email: tengyin811@163.com, jun_zou@njust.edu.cn.

Feng Shu is with the School of Information and Communication Engineering, Hainan University, Haikou, 570228, China, and also with the School of Electronic and Optical Engineering, Nanjing University of Science and Technology, Nanjing, 210094, China, email: shufeng0101@163.com.

J. Wang is with the School of Engineering, University of Kent, Canterbury CT2 7NT, U.K., email: j.z.wang@kent.ac.uk.

F. Shu and M. Huang are corresponding authors.

Digital Object Identifier: 10.23919/JCN.2022.000029.

1229-2370/22/$10.00 © 2022 KICS

cone programming were designed to minimize the transmit power. In [26], based on the Arimoto-Blahut algorithm, the source precoders and IRS phase shift matrix in the full-duplex MIMO two-way communication system were optimized to maximize the sum rate. A fast converging alternating algorithm to maximize the sum rate was proposed in [27]. Compared to the algorithm in [26], the proposed algorithm achieved a faster convergence rate and lower computational complexity. In [28], the convergence analysis for an IRS-aided communication network was presented, and the results revealed that the larger coverage could be provided by using IRS. In [29], the authors proposed to invoke an IRS at the cell boundary of multiple cells to assist the downlink transmission to cell-edge users, and the precoding matrices at the BSs and IRS phase shifts were jointly optimized to maximize the weighted sum rate of all users.

For a continuous phase shift IRS-aided network, it is difficult to implement in practice due to a higher circuit cost than that with finite-phase shifters, especially when the number of elements for IRS tends to large scale. Similar to that discrete-quantized radio frequency phase shifter in directional modulation networks would cause performance loss in [30]–[32], using discrete-phase shifters in IRS will also result in substantial performance loss in IRS-aided wireless network [19], [24], [33]. Choosing a proper number of quantization bits for discrete-phase shifters with a given performance loss will provide a valuable reference for the future system design. Thus, in what follows, we will present an analysis on impact of discrete-phase shifters on the performance of IRS-aided wireless network system in this paper. Our main contributions are summarized as follows:

1) To make an analysis of performance loss caused by discrete-phase shifters, an IRS-aided wireless network is considered. We assume that all channels are LoS channels. Based on the law of large numbers, the closed-form expressions of signal-to-noise ratio (SNR) performance loss, achievable rate (AR), and bit error rate (BER) are successively derived. Simulation results show that the performance losses of SNR and AR gradually decrease as the number of quantization bits increases, while they gradually increase as the number of IRS phase shifter increases. When the number of quantization bits is equal to 3, the performance losses of SNR and AR are respectively less than 0.23 dB and 0.08 bits/s/Hz, and the BER performance degradation is negligible.
2) In the Rayleigh fading channels, with the weak law of large numbers and the Rayleigh distribution, the closed-form expression of SNR performance loss (PL) is derived while AR and BER with PL are given. In addition, based on the Taylor series expansion, the simple approximate performance loss (APL) expression of SNR is derived whereas AR and BER with APL are given. Simulation results show that the SNR, AR and BER PL tendencies in the Rayleigh channels are similar to those in LoS channels. That is, 3-bit phase shifters are sufficient to achieve an omitted performance loss. In particular, the approximate simple expression of performance loss makes a good approximation to the true performance loss when the number of quantization bits is larger than or equal to 2.

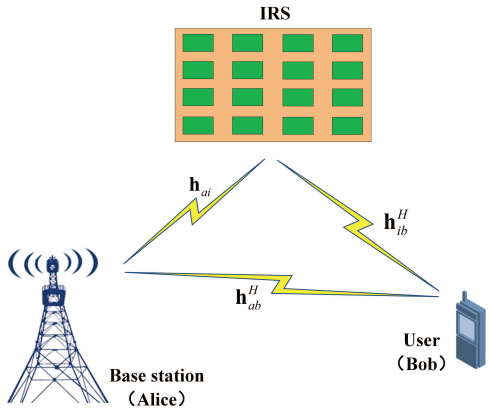

Fig. 1. System model of IRS-aided wireless network.

The remainder of this paper is organized as follows. Section II describes the system model of a typical IRS-aided three-node wireless network. The performance loss derivations in the LoS and Rayleigh channels are presented in Section III and Section IV, respectively. Numerical simulation results are presented in Section V. Finally, we draw conclusions in Section VI.

Notations: throughout this paper, boldface lower case and upper case letters represent vectors and matrices, respectively. Signs $(\cdot)^T$, $(\cdot)^H$, $(\cdot)^{-1}$, $\|\cdot\|_2$, and $|\cdot|$ denote the transpose operation, conjugate transpose operation, inverse operation, 2-norm operation, and absolute value operation, respectively. The symbol $\mathbb{C}^{N\times N}$ denotes the space of $N \times N$ complex-valued matrix. The notation $\mathbf{I}_N$ represents the $N \times N$ identity matrix.

II. SYSTEM MODEL

As shown in Fig. 1, an IRS-aided wireless network system is considered. Herein, the base station (Alice) and user (Bob) are equipped with single antenna. The IRS is equipped with M low-cost passive reflecting elements and reflects signal only one time slot. The Alice→IRS, Alice→Bob, and IRS→Bob channels are the LoS or Rayleigh channels.

The transmit signal at Alice is given by

$$s = \sqrt{P_a}x, \tag{1}$$

where P_a denotes the total transmit power, x is the confidential message and satisfies $\mathbb{E}[\|x\|^2] = 1$.

Taking the path loss into consideration, the received signal at Bob is

$$\begin{aligned} y_b &= \left(\sqrt{g_{aib}}\mathbf{h}_{ib}^H\mathbf{\Theta}\mathbf{h}_{ai} + \sqrt{g_{ab}}\mathbf{h}_{ab}^H\right)s + n_b \\ &= \left(\sqrt{g_{aib}P_a}\mathbf{h}_{ib}^H\mathbf{\Theta}\mathbf{h}_{ai} + \sqrt{g_{ab}P_a}h_{ab}^H\right)x + n_b, \end{aligned} \tag{2}$$

where $g_{aib} = g_{ai}g_{ib}$ represents the equivalent path loss coefficient of Alice→IRS channel and IRS→Bob channel, and g_{ab} is the path loss coefficient of Alice→Bob channel. n_b denotes the

additive white Gaussian noise (AWGN) at Bob with the distribution $\mathcal{CN} \sim (0, \sigma^2)$. $\mathbf{\Theta} = \text{diag}\left(e^{j\phi_1}, \cdots, e^{j\phi_m}, \cdots, e^{j\phi_M}\right)$ represents the diagonal reflection coefficient matrix of IRS, where $\phi_m \in [0, 2\pi)$ denotes the phase shift of reflection element m. $\mathbf{h}_{ai} \in \mathbb{C}^{M\times 1}$, $\mathbf{h}_{ab}^H = h_{ab}^H \in \mathbb{C}^{1\times 1}$, and $\mathbf{h}_{ib}^H \in \mathbb{C}^{1\times M}$ are the Alice→IRS, Alice→Bob, and IRS→Bob channels, respectively.

III. Performance Loss Derivation and Analysis in the LoS Channels

In this section, it is assumed that all channels are the LoS channels. The use of IRS with discrete phase shifters may lead to phase quantization errors. In what follows, we will make a comprehensive investigation of the impact of IRS with discrete phase shifters on SNR, AR, and BER.

Defining $\mathbf{h}_{ai} = \mathbf{h}(\theta_{ai})$, $\mathbf{h}_{ib} = \mathbf{h}(\theta_{ib})$, the steering vector arrival or departure from IRS is

$$\mathbf{h}(\theta) = \left[e^{j2\pi\Psi_\theta(1)}, \cdots, e^{j2\pi\Psi_\theta(m)}, \cdots, e^{j2\pi\Psi_\theta(M)}\right]^T, \quad (3)$$

and the phase function $\Psi_\theta(m)$ is given by

$$\Psi_\theta(m) \triangleq -\frac{(m-(M+1)/2)d\cos\theta}{\lambda}, m = 1, \cdots, M, \quad (4)$$

where m denotes the m-th antenna, d is the spacing of adjacent transmitting antennas, θ represents the direction angle of arrival or departure, and λ represents the wavelength.

The receive signal (2) can be casted as

$$\begin{aligned} y_b^{LoS} &= \left(\sqrt{g_{aib}P_a}\mathbf{h}^H(\theta_{ib})\mathbf{\Theta}\mathbf{h}(\theta_{ai}) + \sqrt{g_{ab}P_a}h_{ab}^H\right)x + n_b \\ &= \sqrt{g_{aib}P_a}\left(\sum_{m=1}^{M} e^{j\left(-2\pi\Psi_{\theta_{ib}}(m)+\phi_m+2\pi\Psi_{\theta_{ai}}(m)\right)}\right)x \\ &\quad + \sqrt{g_{ab}P_a}|h_{ab}|e^{-j\varphi_{ab}}x + n_b \\ &= \sqrt{g_{aib}P_a}e^{-j\varphi_{ab}} \\ &\quad \times \left[\left(\sum_{m=1}^{M} e^{j(-2\pi\Psi_{\theta_{ib}}(m)+\phi_m+2\pi\Psi_{\theta_{ai}}(m)+\varphi_{ab})}\right)\right. \\ &\quad \left. + \sqrt{g_{ab}P_a}|h_{ab}|\right]x + n_b, \end{aligned} \quad (5)$$

where φ_{ab} is the phase of h_{ab}.

As shown above, considering we only adjust the phases of IRS elements, if all IRS phases are adjusted to have the same phase as that of LoS path, then all $(M+1)$-path signals form a constructive combining at Bob. If the phase shifter at IRS is continuous, and the transmit signal at Alice is forwarded perfectly to Bob by the IRS, the m-th phase shift at IRS can be designed as follows

$$\phi_m = 2\pi\Psi_{\theta_{ib}}(m) - 2\pi\Psi_{\theta_{ai}}(m) - \varphi_{ab}. \quad (6)$$

In what follows, for convenience of deriving, φ_{ab} is chosen to be zero. Then (5) can be converted to

$$y_b^{LoS} = \sqrt{g_{aib}P_a}Mx + \sqrt{g_{ab}P_a}|h_{ab}|x + n_b. \quad (7)$$

A. Derivation of Performance Loss in LoS Channels

Assuming the discrete phase shifters is employed by IRS, and the discrete phases per phase shifters at IRS employs a k-bit phase quantizer, each reflection element's phase feasible set is

$$\Omega = \left\{\frac{\pi}{2^k}, \frac{3\pi}{2^k}, \cdots, \frac{(2^{k+1}-1)\pi}{2^k}\right\}. \quad (8)$$

Assuming that ϕ_m is the desired continuous phase of the m-th element at IRS, and the final discrete phase is chosen from phase feasible set Ω, which is given by

$$\overline{\phi_m} = \arg\min_{\overline{\phi_m}\in\Omega} \|\overline{\phi_m} - \phi_m\|_2. \quad (9)$$

In general, $\overline{\phi_m} \neq \phi_m$, which means that phase mismatching may lead to performance loss at Bob. Let us define the m-th phase quantization error at IRS as follows

$$\Delta\phi_m = \overline{\phi_m} - \phi_m. \quad (10)$$

It is assumed that the above phase quantization error follows uniform distribution with probability density function (PDF) as follows

$$f(x) = \begin{cases} \frac{1}{2\Delta x}, & x \in [-\Delta x, \Delta x], \\ 0, & \text{otherwise}, \end{cases} \quad (11)$$

where

$$\Delta x = \frac{\pi}{2^k}. \quad (12)$$

In the presence of phase quantization error, the receive signal (2) becomes

$$\begin{aligned} \widehat{y_b}^{LoS} &= \left(\sqrt{g_{aib}P_a}\mathbf{h}^H(\theta_{ib})\mathbf{\Theta}\mathbf{h}(\theta_{ai}) + \sqrt{g_{ab}P_a}h_{ab}^H\right)x + n_b \\ &= \sqrt{g_{aib}P_a}\left(\sum_{m=1}^{M} e^{j\left(-2\pi\Psi_{\theta_{ib}}(m)+\overline{\phi_m}+2\pi\Psi_{\theta_{ai}}(m)\right)}\right)x \\ &\quad + \sqrt{g_{ab}P_a}|h_{ab}|x + n_b \\ &= \sqrt{g_{aib}P_a}\left(\sum_{m=1}^{M} e^{j\Delta\phi_m}\right)x + \sqrt{g_{ab}P_a}|h_{ab}|x + n_b. \end{aligned} \quad (13)$$

Observing the above equation, it is apparently that if and only if $\Delta\phi_m = 0$, the phase alignment at user is achieved to realize the optimal coherent combining gain M^2. Due to the use of finite phase shifting, in general, $\Delta\phi_m$ is random and is unequal to zero, this means that the combining gain is lower than or far less than M^2. In other words, the receive performance decays.

In accordance with the law of large numbers in [34] and (11), we can obtain

$$\begin{aligned} \frac{1}{M}\sum_{m=1}^{M} e^{j\Delta\phi_m} &\approx \mathbb{E}\left(e^{j\Delta\phi_m}\right) \\ &= \int_{-\Delta x}^{\Delta x} e^{j\Delta\phi_m} f\left(\Delta\phi_m\right) d\left(\Delta\phi_m\right) \\ &= \int_{-\Delta x}^{\Delta x} \frac{e^{j\Delta\phi_m}}{2\Delta x} d\left(\Delta\phi_m\right) \\ &= \frac{1}{2\Delta x}\int_{-\Delta x}^{\Delta x} \cos\left(\Delta\phi_m\right) d\left(\Delta\phi_m\right). \end{aligned} \quad (14)$$

A further simplification of (14) yields

$$\begin{aligned}\frac{1}{M}\sum_{m=1}^{M} e^{j\Delta\phi_m} &\approx \frac{1}{2\Delta x}\int_{-\Delta x}^{\Delta x}\cos\left(\Delta\phi_m\right)d\left(\Delta\phi_m\right)\\ &= \frac{1}{2\Delta x}\cdot 2\sin(\Delta x)\\ &= \frac{\sin(\Delta x)}{\Delta x}\\ &= \text{sinc}\left(\frac{\pi}{2^k}\right).\end{aligned} \tag{15}$$

Plugging (15) in (13) yields

$$\widehat{y_b}^{LoS} \approx \sqrt{g_{aib}P_a}M\text{sinc}\left(\frac{\pi}{2^k}\right)x + \sqrt{g_{ab}P_a}|h_{ab}|x + n_b. \tag{16}$$

In what follows, to simplify (16), we consider that the number of quantization bits is large, that is, $\Delta\phi_m$ goes to zero. Using the Taylor series expansion [35], we have the following approximation

$$\cos\left(\Delta\phi_m\right) \approx 1 - \frac{\Delta\phi_m^2}{2}, \tag{17}$$

then (14) can be rewritten as

$$\begin{aligned}\frac{1}{M}\sum_{m=1}^{M} e^{j\Delta\phi_m} &\approx \frac{1}{2\Delta x}\int_{-\Delta x}^{\Delta x}\cos\left(\Delta\phi_m\right)d\left(\Delta\phi_m\right)\\ &\approx \frac{1}{2\Delta x}\int_{-\Delta x}^{\Delta x}\left(1-\frac{\Delta\phi_m^2}{2}\right)d\left(\Delta\phi_m\right)\\ &= \frac{1}{2\Delta x}\left(2\Delta x - \frac{1}{3}(\Delta x)^3\right)\\ &= 1-\frac{1}{6}\left(\frac{\pi}{2^k}\right)^2.\end{aligned} \tag{18}$$

At this point, the receive signal at Bob under the approximate phase quantization error is

$$\begin{aligned}\widetilde{y_b}^{LoS} \approx &\sqrt{g_{aib}P_a}\left(1-\frac{1}{6}\left(\frac{\pi}{2^k}\right)^2\right)Mx\\ &+\sqrt{g_{ab}P_a}|h_{ab}|x + n_b.\end{aligned} \tag{19}$$

B. Performance Loss of SNR at Bob

In accordance with (7), the SNR expression with no PL, i.e., $k \to \infty$, is given by

$$\text{SNR}^{LoS} = \frac{\left(\sqrt{g_{aib}P_a}M + \sqrt{g_{ab}P_a}|h_{ab}|\right)^2}{\sigma^2}. \tag{20}$$

From (16) and (19), the expressions of the SNR with PL and approximate PL are

$$\widehat{\text{SNR}}^{LoS} = \frac{\left(\sqrt{g_{aib}P_a}M\text{sinc}\left(\frac{\pi}{2^k}\right) + \sqrt{g_{ab}P_a}|h_{ab}|\right)^2}{\sigma^2}, \tag{21}$$

and

$$\widetilde{\text{SNR}}^{LoS} = \frac{\left(\sqrt{g_{aib}P_a}\left(1-\frac{1}{6}\left(\frac{\pi}{2^k}\right)^2\right)M + \sqrt{g_{ab}P_a}|h_{ab}|\right)^2}{\sigma^2}, \tag{22}$$

respectively, where k is a finite positive integer.

Then the SNR PL and APL are given by

$$\begin{aligned}\widehat{L}^{LoS} &= \frac{\text{SNR}^{LoS}}{\widehat{\text{SNR}}^{LoS}}\\ &= \frac{\left(\sqrt{g_{aib}}M + \sqrt{g_{ab}}|h_{ab}|\right)^2}{\left(\sqrt{g_{aib}}M\text{sinc}\left(\frac{\pi}{2^k}\right) + \sqrt{g_{ab}}|h_{ab}|\right)^2}\\ &= \left(1 + \frac{\sqrt{g_{aib}}\left(1-\text{sinc}\left(\frac{\pi}{2^k}\right)\right)}{\sqrt{g_{aib}}\text{sinc}\left(\frac{\pi}{2^k}\right) + \frac{1}{M}\sqrt{g_{ab}}|h_{ab}|}\right)^2,\end{aligned} \tag{23}$$

and

$$\begin{aligned}\widetilde{L}^{LoS} &= \frac{\text{SNR}^{LoS}}{\widetilde{\text{SNR}}^{LoS}}\\ &= \frac{\left(\sqrt{g_{aib}}M + \sqrt{g_{ab}}|h_{ab}|\right)^2}{\left(\sqrt{g_{aib}}\left(1-\frac{1}{6}\left(\frac{\pi}{2^k}\right)^2\right)M + \sqrt{g_{ab}}|h_{ab}|\right)^2}\\ &= \left(1 + \frac{\sqrt{g_{aib}}\cdot\frac{1}{6}\left(\frac{\pi}{2^k}\right)^2}{\sqrt{g_{aib}}\left(1-\frac{1}{6}\left(\frac{\pi}{2^k}\right)^2\right) + \frac{1}{M}\sqrt{g_{ab}}|h_{ab}|}\right)^2,\end{aligned} \tag{24}$$

respectively. From (23), (24), and k being a finite positive integer, it can be found that $\widehat{L}^{LoS}$ and $\widetilde{L}^{LoS}$ gradually decrease as k increases, while they gradually increase as M increases.

C. Performance Loss of Achievable Rate at Bob

According to (7), (16), and (19), the achievable rate at Bob with no PL, PL, and APL are given by

$$R^{LoS} = \log_2\left(1 + \frac{\left(\sqrt{g_{aib}P_a}M + \sqrt{g_{ab}P_a}|h_{ab}|\right)^2}{\sigma^2}\right), \tag{25}$$

$$\widehat{R}^{LoS} = \log_2\left(1 + \frac{\left(\sqrt{g_{aib}P_a}M\text{sinc}\left(\frac{\pi}{2^k}\right) + \sqrt{g_{ab}P_a}|h_{ab}|\right)^2}{\sigma^2}\right), \tag{26}$$

and

$$\widetilde{R}^{LoS} = \log_2\left(1 + \frac{\left(\sqrt{g_{aib}P_a}\left(1-\frac{1}{6}\left(\frac{\pi}{2^k}\right)^2\right)M + \sqrt{g_{ab}P_a}|h_{ab}|\right)^2}{\sigma^2}\right), \tag{27}$$

respectively.

D. Performance Loss of BER at Bob

In accordance with [34], the expression of BER is

$$\text{BER}(z) \approx \beta Q\left(\sqrt{\mu z}\right), \tag{28}$$

where β and μ depend on the type of approximation and the modulation type, β represents the number of nearest neighbors to a constellation at the minimum distance, and μ is a constant that is related to minimum distance to average symbol energy, z denotes the SNR per symbol, $Q(z)$ represents the probability

that a Gaussian random variable x with mean zero and variance one exceeds the value z, i.e.,

$$Q(z) = \int_z^{+\infty} \frac{1}{\sqrt{2\pi}} e^{\frac{-x^2}{2}} dx. \tag{29}$$

Assuming the quadrature phase shift keying (QPSK) is employed as the modulation scheme, according to (7), (16), and (19), the BERs at Bob with no PL, PL, and APL are given by

$$\text{BER}^{LoS} \approx Q\left(\sqrt{\frac{\left(\sqrt{g_{aib}P_a}M + \sqrt{g_{ab}P_a}|h_{ab}|\right)^2}{\sigma^2}}\right), \tag{30}$$

$$\widehat{\text{BER}}^{LoS} \approx Q\left(\sqrt{\frac{\left(\sqrt{g_{aib}P_a}M\text{sinc}\left(\frac{\pi}{2^k}\right) + \sqrt{g_{ab}P_a}|h_{ab}|\right)^2}{\sigma^2}}\right), \tag{31}$$

and

$$\widetilde{\text{BER}}^{LoS} \approx Q\left(\sqrt{\frac{\left(\sqrt{g_{aib}P_a}\left(1 - \frac{1}{6}\left(\frac{\pi}{2^k}\right)^2\right)M + \sqrt{g_{ab}P_a}|h_{ab}|\right)^2}{\sigma^2}}\right), \tag{32}$$

respectively. This completes the derivations of the corresponding SNR performance loss, ARs and BERs with PL and APL in LoS channels.

IV. Performance Loss Derivation and Analysis in the Rayleigh Channels

In this section, we make an analysis of the impact of discrete phase shift of IRS on SNR, AR, and BER. The corresponding closed-form expressions of SNR performance loss, AR, and BER are derived in the Rayleigh fading channels.

A. Derivation of Performance Loss in the Rayleigh Channels

Assuming all channels are Rayleigh channels obeying the Rayleigh distribution, the corresponding PDF is as follows

$$f_\alpha(x) = \begin{cases} \frac{x}{\alpha^2} e^{-\frac{x^2}{2\alpha^2}}, & x \in [0, +\infty), \\ 0, & \text{otherwise}, \end{cases} \tag{33}$$

where $\alpha > 0$ represents the Rayleigh distribution parameter.

Assuming discrete phase shifters is employed by IRS, there is a phase quantization error due to the effect of phase mismatching, i.e., $\Delta\phi_m \neq 0$, then the performance loss is incurred. Due to the phase mismatching of discrete phase shifters in IRS, the receive signal (2) can be rewritten as

$$\begin{aligned}
\widehat{y}_b^{RL} &= \left(\sqrt{g_{aib}P_a}\mathbf{h}_{ib}^H\mathbf{\Theta}\mathbf{h}_{ai} + \sqrt{g_{ab}P_a}h_{ab}^H\right)x + n_b \\
&= \Big(\sqrt{g_{aib}P_a}\sum_{m=1}^{M}(|h_{ib}(m)||h_{ai}(m)|e^{j\Delta\phi_m}) \\
&\quad + \sqrt{g_{ab}P_a}|h_{ab}|\Big)x + n_b \\
&= \Big(\sqrt{g_{aib}P_a}\Big(\underbrace{M \cdot \frac{1}{M}\sum_{m=1}^{M}(|h_{ib}(m)||h_{ai}(m)|\cos(\Delta\phi_m))}_{W} + \\
&\quad \underbrace{jM \cdot \frac{1}{M}\sum_{m=1}^{M}(|h_{ib}(m)||h_{ai}(m)|\sin(\Delta\phi_m))}_{G}\Big) + \\
&\quad \sqrt{g_{ab}P_a}\mathbb{E}(|h_{ab}|)\Big)x + n_b.
\end{aligned} \tag{34}$$

Using the weak law of large numbers, and the fact that $|h_{ai}(m)|$ and $|h_{ib}(m)|$ are independently identically distributed Rayleigh distributions with parameters α_{ai} and α_{ib}, respectively, and their elements are independent of each other, we have

$$\begin{aligned}
G &\approx \mathbb{E}(|h_{ib}(m)||h_{ai}(m)|\sin(\Delta\phi_m)) \\
&= \iiint |h_{ib}(m)||h_{ai}(m)|\sin(\Delta\phi_m) f_{\alpha_{ib}}(|h_{ib}(m)|) \bullet \\
&\quad f_{\alpha_{ai}}(|h_{ai}(m)|) f(\sin(\Delta\phi_m)) d(\Delta\phi_m) d(|h_{ai}(m)|) \bullet \\
&\quad d(|h_{ib}(m)|).
\end{aligned} \tag{35}$$

Since $|h_{ib}(m)|$, $|h_{ai}(m)|$, and $\sin(\Delta\phi_m)$ are independent of each other, (35) can be further converted to

$$\begin{aligned}
G &\approx \int_0^{+\infty} |h_{ib}(m)| f_{\alpha_{ib}}(|h_{ib}(m)|) \int_0^{+\infty} |h_{ai}(m)| \bullet \\
&\quad f_{\alpha_{ai}}(|h_{ai}(m)|) \int_{-\Delta x}^{\Delta x} \sin(\Delta\phi_m) f(\Delta\phi_m)) d(\Delta\phi_m) \bullet \\
&\quad d(|h_{ai}(m)|) d(|h_{ib}(m)|) \\
&= 0.
\end{aligned} \tag{36}$$

Due to the fact that $|h_{ib}(m)|$, $|h_{ai}(m)|$, and $\cos(\Delta\phi_m)$ are also independent of each other, similar to the derivation of (35) and (36), we have

$$\begin{aligned}
W &= \frac{1}{M}\sum_{m=1}^{M}(|h_{ib}(m)||h_{ai}(m)|\cos(\Delta\phi_m)) \\
&\approx \mathbb{E}(|h_{ib}(m)||h_{ai}(m)|\cos(\Delta\phi_m)) \\
&= \int_0^{+\infty} |h_{ib}(m)| f_{\alpha_{ib}}(|h_{ib}(m)|) \int_0^{+\infty} |h_{ai}(m)| \bullet \\
&\quad f_{\alpha_{ai}}(|h_{ai}(m)|) \int_{-\Delta x}^{\Delta x} \cos(\Delta\phi_m) f(\Delta\phi_m) d(\Delta\phi_m) \bullet \\
&\quad d(|h_{ai}(m)|) d(|h_{ib}(m)|) \\
&= \text{sinc}\left(\frac{\pi}{2^k}\right) \int_0^{+\infty} |h_{ib}(m)| f_{\alpha_{ib}}(|h_{ib}(m)|) \int_0^{+\infty} |h_{ai}(m)| \\
&\quad \bullet f_{\alpha_{ai}}(|h_{ai}(m)|) d(|h_{ai}(m)|) d(|h_{ib}(m)|) \\
&= \text{sinc}\left(\frac{\pi}{2^k}\right)\frac{\pi}{2}\alpha_{ai}\alpha_{ib}.
\end{aligned} \tag{37}$$

Plugging (36) and (37) into (34) yields

$$\widehat{y}_b^{RL} \approx \left(\sqrt{g_{aib}P_a}M\text{sinc}\left(\frac{\pi}{2^k}\right)\frac{\pi}{2}\alpha_{ai}\alpha_{ib}+\sqrt{\frac{g_{ab}P_a\pi}{2}}\alpha_{ab}\right)x + n_b, \tag{38}$$

where α_{ab} is the Rayleigh distribution parameter of channel from Alice to Bob.

To simplify (38), in terms of (17) and the fact that $|h_{ib}|$, $|h_{ai}|$, and $\Delta\phi_m^2$ are independent of each other, we can obtain

$$\begin{aligned}
W &\approx \frac{1}{M}\sum_{m=1}^{M}|h_{ib}(m)|\,|h_{ai}(m)|\left(1-\frac{\Delta\phi_m^2}{2}\right)\\
&= \frac{1}{M}\sum_{m=1}^{M}|h_{ib}(m)|\,|h_{ai}(m)| - \frac{1}{M}\sum_{m=1}^{M}|h_{ib}(m)|\bullet\\
&\quad |h_{ai}(m)|\,\frac{\Delta\phi_m^2}{2}\\
&= \mathbb{E}\left(|h_{ib}(m)|\,|h_{ai}(m)|\right) - \mathbb{E}\left(|h_{ib}(m)|\,|h_{ai}(m)|\,\frac{\Delta\phi_m^2}{2}\right)\\
&= \int_0^{+\infty}|h_{ib}(m)|f_{\alpha_{ib}}\left(|h_{ib}(m)|\right)\int_0^{+\infty}|h_{ai}(m)|\bullet\\
&\quad f_{\alpha_{ai}}(|h_{ai}(m)|)d\left(|h_{ai}(m)|\right)d\left(|h_{ib}(m)|\right) - \int_0^{+\infty}|h_{ib}(m)|\\
&\quad \bullet f_{\alpha_{ib}}\left(|h_{ib}(m)|\right)\int_0^{+\infty}|h_{ai}(m)|f_{\alpha_{ai}}\left(|h_{ai}(m)|\right)\int_{-\Delta x}^{\Delta x}\\
&\quad \bullet \frac{\Delta\phi_m^2}{2}f\left(\Delta\phi_m\right))\,d\left(\Delta\phi_m\right)d\left(|h_{ai}(m)|\right)d\left(|h_{ib}(m)|\right)\\
&= \frac{\pi}{2}\alpha_{ai}\alpha_{ib} - \frac{1}{6}\left(\frac{\pi}{2^k}\right)^2\frac{\pi}{2}\alpha_{ai}\alpha_{ib}\\
&= \left(1-\frac{1}{6}\left(\frac{\pi}{2^k}\right)^2\right)\frac{\pi}{2}\alpha_{ai}\alpha_{ib}.
\end{aligned} \tag{39}$$

Plugging (39) into (34) yields

$$\widetilde{y}_b^{RL} \approx \left(\sqrt{g_{aib}P_a}M\left(1-\frac{1}{6}\left(\frac{\pi}{2^k}\right)^2\right)\frac{\pi}{2}\alpha_{ai}\alpha_{ib}+\sqrt{\frac{g_{ab}P_a\pi}{2}}\alpha_{ab}\right)x + n_b. \tag{40}$$

Assuming there is no quantization error, i.e., $\Delta\phi_m = 0$, the receive signal (38) degrades to

$$y_b^{RL} = \left(\sqrt{g_{aib}P_a}M\frac{\pi}{2}\alpha_{ai}\alpha_{ib}+\sqrt{\frac{g_{ab}P_a\pi}{2}}\alpha_{ab}\right)x + n_b. \tag{41}$$

B. Performance Loss of SNR at Bob

Based on (41), (38), and (40), the SNR expressions of no PL, PL, and APL are given by

$$\text{SNR}^{RL} = \frac{\left(\sqrt{g_{aib}P_a}M\frac{\pi}{2}\alpha_{ai}\alpha_{ib}+\sqrt{\frac{g_{ab}P_a\pi}{2}}\alpha_{ab}\right)^2}{\sigma^2}, \tag{42}$$

$$\widehat{\text{SNR}}^{RL} = \frac{\left(\sqrt{g_{aib}P_a}M\text{sinc}\left(\frac{\pi}{2^k}\right)\frac{\pi}{2}\alpha_{ai}\alpha_{ib}+\sqrt{\frac{g_{ab}P_a\pi}{2}}\alpha_{ab}\right)^2}{\sigma^2}, \tag{43}$$

and

$$\widetilde{\text{SNR}}^{RL} = \frac{\left(\sqrt{g_{aib}P_a}M\left(1-\frac{1}{6}\left(\frac{\pi}{2^k}\right)^2\right)\frac{\pi}{2}\alpha_{ai}\alpha_{ib}+\sqrt{\frac{g_{ab}P_a\pi}{2}}\alpha_{ab}\right)^2}{\sigma^2}, \tag{44}$$

respectively.

Then the SNR PL and APL are given as

$$\begin{aligned}
\widehat{L}^{RL} &= \frac{\text{SNR}^{RL}}{\widehat{\text{SNR}}^{RL}}\\
&= \frac{\left(\sqrt{g_{aib}}M\frac{\pi}{2}\alpha_{ai}\alpha_{ib}+\sqrt{\frac{g_{ab}\pi}{2}}\alpha_{ab}\right)^2}{\left(\sqrt{g_{aib}}M\text{sinc}\left(\frac{\pi}{2^k}\right)\frac{\pi}{2}\alpha_{ai}\alpha_{ib}+\sqrt{\frac{g_{ab}\pi}{2}}\alpha_{ab}\right)^2}\\
&= \left(1+\frac{\sqrt{g_{aib}}\frac{\pi}{2}\alpha_{ai}\alpha_{ib}\left(1-\text{sinc}\left(\frac{\pi}{2^k}\right)\right)}{\sqrt{g_{aib}}\text{sinc}\left(\frac{\pi}{2^k}\right)\frac{\pi}{2}\alpha_{ai}\alpha_{ib}+\frac{1}{M}\sqrt{\frac{g_{ab}\pi}{2}}\alpha_{ab}}\right)^2,
\end{aligned} \tag{45}$$

and

$$\begin{aligned}
\widetilde{L}^{RL} &= \frac{\text{SNR}^{RL}}{\widetilde{\text{SNR}}^{RL}}\\
&= \frac{\left(\sqrt{g_{aib}}M\frac{\pi}{2}\alpha_{ai}\alpha_{ib}+\sqrt{\frac{g_{ab}\pi}{2}}\alpha_{ab}\right)^2}{\left(\sqrt{g_{aib}}M\left(1-\frac{1}{6}\left(\frac{\pi}{2^k}\right)^2\right)\frac{\pi}{2}\alpha_{ai}\alpha_{ib}+\sqrt{\frac{g_{ab}\pi}{2}}\alpha_{ab}\right)^2}\\
&= \left(1+\frac{\sqrt{g_{aib}}\frac{1}{6}\left(\frac{\pi}{2^k}\right)^2\frac{\pi}{2}\alpha_{ai}\alpha_{ib}}{\sqrt{g_{aib}}\left(1-\frac{1}{6}\left(\frac{\pi}{2^k}\right)^2\right)\frac{\pi}{2}\alpha_{ai}\alpha_{ib}+\frac{1}{M}\sqrt{\frac{g_{ab}\pi}{2}}\alpha_{ab}}\right)^2,
\end{aligned} \tag{46}$$

respectively. Observing (45) and (46), we can find two tendencies: both of $\widehat{L}^{RL}$ and $\widetilde{L}^{RL}$ gradually decrease as k increases, while they gradually increase with increases in the value of M.

C. Performance Loss of Achievable Rate at Bob

In accordance with (41), (38), and (40), the achievable rates at Bob in the absence of PL, in the presence of PL and APL are given by

$$R^{RL} = \log_2\left(1+\frac{\left(\sqrt{g_{aib}P_a}M\frac{\pi}{2}\alpha_{ai}\alpha_{ib}+\sqrt{\frac{g_{ab}P_a\pi}{2}}\alpha_{ab}\right)^2}{\sigma^2}\right), \tag{47}$$

$$\widehat{R}^{RL} = \log_2\left(1+\frac{\left(\sqrt{g_{aib}P_a}M\text{sinc}\left(\frac{\pi}{2^k}\right)\frac{\pi}{2}\alpha_{ai}\alpha_{ib}+\sqrt{\frac{g_{ab}P_a\pi}{2}}\alpha_{ab}\right)^2}{\sigma^2}\right), \tag{48}$$

and

$$\widetilde{R}^{RL} = \log_2\left(1+ \frac{\left(\sqrt{g_{aib}P_a}M\left(1-\frac{1}{6}\left(\frac{\pi}{2^k}\right)^2\right)\frac{\pi}{2}\alpha_{ai}\alpha_{ib}+\sqrt{\frac{g_{ab}P_a\pi}{2}}\alpha_{ab}\right)^2}{\sigma^2}\right), \tag{49}$$

respectively.

D. Performance Loss of BER at Bob

From (41), (38), and (40), when the QPSK modulation is assumed to be employed, the BERs at Bob with no PL, PL, and APL are given by

$$\mathrm{BER}^{RL} \approx Q\left(\sqrt{\frac{\left(\sqrt{g_{aib}P_a}M\frac{\pi}{2}\alpha_{ai}\alpha_{ib}+\sqrt{\frac{g_{ab}P_a\pi}{2}}\alpha_{ab}\right)^2}{\sigma^2}}\right), \tag{50}$$

$$\widehat{\mathrm{BER}}^{RL} \approx Q\left(\sqrt{\frac{\left(\sqrt{g_{aib}P_a}M\,\mathrm{sinc}\left(\frac{\pi}{2^k}\right)\frac{\pi}{2}\alpha_{ai}\alpha_{ib}+\sqrt{\frac{g_{ab}P_a\pi}{2}}\alpha_{ab}\right)^2}{\sigma^2}}\right), \tag{51}$$

and

$$\widetilde{\mathrm{BER}}^{RL} \approx Q\left(\sqrt{\frac{P_a\left(\sqrt{g_{aib}}M\left(1-\frac{1}{6}\left(\frac{\pi}{2^k}\right)^2\right)\frac{\pi}{2}\alpha_{ai}\alpha_{ib}+\sqrt{\frac{g_{ab}\pi}{2}}\alpha_{ab}\right)^2}{\sigma^2}}\right), \tag{52}$$

respectively. It is noted that the above derived results may be extended to the scenarios of high-order digital modulations like M-ary phase shift keying (MPSK), M-ary quadrature amplitude modulation (MQAM).

V. Simulation Results and Discussions

In this section, the simulation results are presented to evaluate the effect of phase mismatching caused by IRS with discrete phase shifters from three different aspects: SNR, AR, and BER. The path loss at the distance $\bar{d}$ is modeled as $g(\bar{d}) = \mathrm{PL}_0 - 10\gamma\log_{10}\bar{d}/d_0$, where $\mathrm{PL}_0 = -30$ dB represents the path loss reference distance $d_0 = 1$ m, and γ is the path loss exponent. The path loss exponents of Alice→IRS, IRS→Bob, and Alice→Bob channels are respectively chosen as 2, 2, and 2 in the LoS channels, and the one are respectively set to be 2.5, 2.5, and 3.5 in the Rayleigh channels. The default system parameters are chosen as follows: $M = 128$, $d = \lambda/2$, $\theta_{ab} = \pi/2$, $\theta_{ai} = \pi/4$, $d_{ab} = 100$ m, $d_{ai} = 30$ m, $P_a = 30$ dBm. $\alpha_{ai} = \alpha_{ib} = \alpha_{ab} = 0.5$.

Figs. 2 (a) and (b) plot the curves of SNR performance loss versus the number k of quantization bits ranging from 1 to 6 in LoS and Rayleigh channels, respectively, where three different IRS element numbers M are chosen: 8, 64 and 1024. It can be seen from the two subfigures that regardless of the case of performance loss (PL) or APL, the SNR performance loss in the LoS channels and Rayleigh channels decreases as the number of quantization bits k increases, while it increases with M increases. They coincide with the conclusions of the theoretical analysis in Sections III and IV. In addition, when k is larger than or equal to 3, the SNR performance loss is less than 0.23 dB even when the number of IRS phase shift elements M tends to large scale (e.g., $M = 1024$). This means that 3 bits is sufficient to achieve a trivial performance loss.

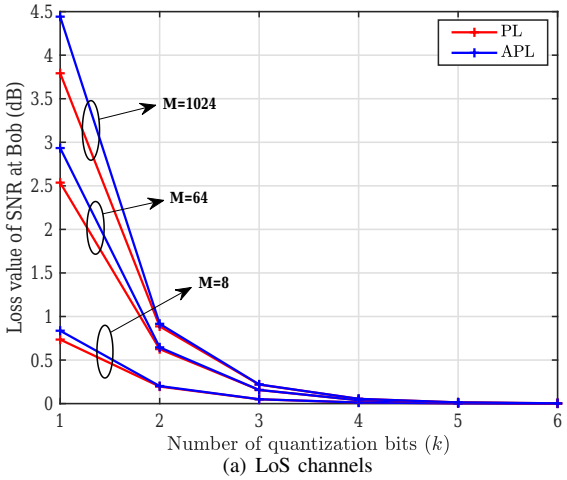

(a) LoS channels

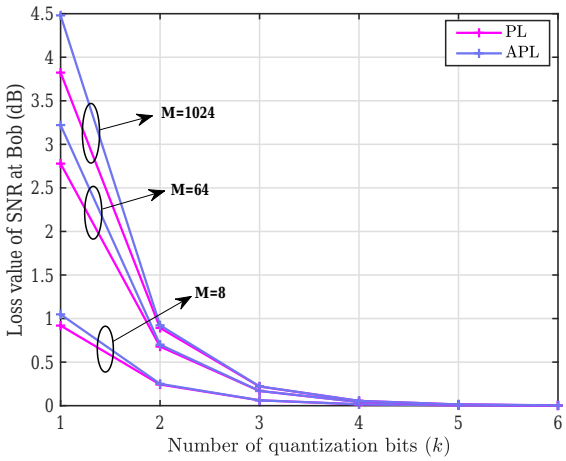

(b) Rayleigh channels

Fig. 2. Curves of loss of SNR versus the number k of quantization bits.

Figs. 3 (a) and (b) show the curves of AR versus the number k of quantization bits ranging from 1 to 6 in LoS and Rayleigh channels, respectively, where the SNR is equal to 15 dB. From Fig. 3, it is seen that the AR performance loss at Bob decreases as k increases, and increases as M increases. Additionally, the AR increases as the number of IRS phase shift elements M increases. Compared with the case of no PL, 3 quantization bits achieves a AR performance loss less than 0.08 bits/s/Hz in the cases of PL and APL regardless of the number of IRS phase shift elements. When the number of quantization bits is

larger than or equal to 2, the simple APL expression coincides with the true PL.

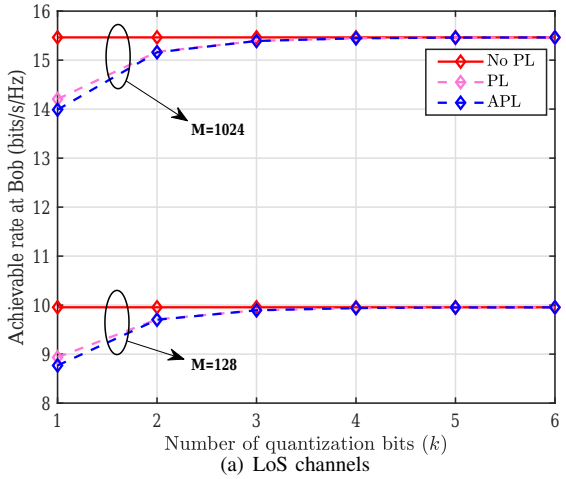

(a) LoS channels

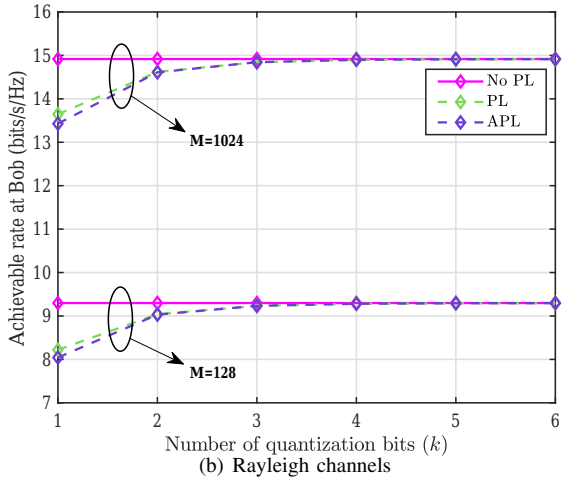

(b) Rayleigh channels

Fig. 3. Curves of AR versus the number k of quantization bits.

Fig. 4 illustrates the curves of BER versus the number k of quantization bits from 1 to 6, where SNR is equal to -5 dB. From Fig. 4, it can be seen that with increasing the number k of quantization bits, the BER performances of PL and APL rapidly approach that no PL. When k reaches up to 3, the BER performances of PL and APL are almost identical to that of no PL, which means that it is feasible in practice to use discrete phase shifters with $k = 3$ to achieve a trivial performance loss. This dramatically reduces the circuit cost and the required CSI amount fed back from BS or user.

VI. Conclusion

In this paper, the performance of IRS with discrete phase shifters of wireless network has been investigated. To make an analysis of the performance loss caused by IRS with phase quantization error, we considered two scenarios: LoS and Rayleigh channels. The closed-form expressions of SNR PL, AR, and BER with PL were derived using the law of large numbers and some mathematic approximation techniques. With the help of the Taylor series expansion, the simple approximate performance loss expressions of IRS with approximate quantization error were also provided. Simulation results showed that when the number of quantization bits is larger than or equal to 3, the performance losses of SNR and AR are less than 0.23 dB and 0.08 bits/s/Hz, respectively, and the corresponding degradation on BER is negligible. The simple approximate expression approaches the true performance loss when the number of quantization bits is larger than or equal to 2.

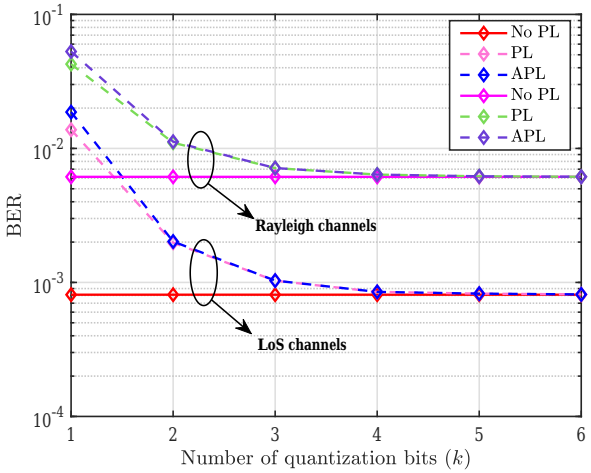

Fig. 4. Curves of BER versus the number k of quantization bits.

References

[1] V. Nguyen, T. P. Truong, T. M. T. Nguyen, W. Noh, and S. Cho, "Achievable rate analysis of two-hop interference channel with coordinated IRS relay," *IEEE Trans. Wireless Commun.*, pp. 1–1, 2022.

[2] Q. Wu and R. Zhang, "Towards smart and reconfigurable environment: Intelligent reflecting surface aided wireless network," *IEEE Commun Mag*, vol. 58, no. 1, pp. 106–112, Jan. 2020.

[3] W. Tang *et al.*, "MIMO transmission through reconfigurable intelligent surface: System design, analysis, and implementation," *IEEE J. Sel. Areas Commun.*, vol. 38, no. 11, pp. 2683–2699, Nov. 2020.

[4] Y. Gao *et al.*, "Reflection resource management for intelligent reflecting surface aided wireless networks," *IEEE Trans. Commun.*, vol. 69, no. 10, pp. 6971–6986, Oct. 2021.

[5] C. Huang, A. Zappone, G. C. Alexandropoulos, M. Debbah, and C. Yuen, "Reconfigurable intelligent surfaces for energy efficiency in wireless communication," *IEEE Trans. Wireless Commun.*, vol. 18, no. 8, pp. 4157–4170, Aug. 2019.

[6] X. Guan, Q. Wu, and R. Zhang, "Intelligent reflecting surfaces assisted secrecy commuincation: Is artificial noise helpful or not?" *IEEE Wireless Commun. Lett.*, vol. 9, no. 6, pp. 778–782, Jun. 2020.

[7] R. Dong *et al.*, "Beamforming and power allocation for double-RIS-aided two-way directional modulation network," [online] Available: https://arxiv.org/abs/2201.09063.

[8] S. Hong, C. Pan, H. Ren, K. Wang, and A. Nallanathan, "Artificial-noise-aided secure MIMO wireless communications via intelligent reflecting surface," *IEEE Trans. Commun.*, vol. 68, no. 12, pp. 7851–7866, Dec. 2020.

[9] X. Wang *et al.*, "Beamforming design for IRS-aided decode-and-forward relay wireless network," *IEEE Trans. Green Commun. Netw.*, vol. 6, no. 1, pp. 198–207, Mar. 2022.

[10] L. Yang, W. Guo, and I. S. Ansari, "Mixed dual-hop FSO-RF communication systems through reconfigurable intelligent surface," *IEEE Commun. Lett.*, vol. 24, no. 7, pp. 1558–1562, Jul. 2020.

[11] Q. Zhu, Y. Gao, Y. Xiao, and S. Mumtaz, "Intelligent reflecting surface aided wireless networks: Dynamic user access and system sum-rate maximization," *IEEE Trans. Commun.*, pp. 1–1, 2022.

[12] A.-H. Ahmed, M. Samir, M. Elhattab, C. Assi, and S. Sharafeddine, "Reconfigurable intelligent surface enabled vehicular communication: Joint user scheduling and passive beamforming," *IEEE Trans. Veh. Technol.*, vol. 71, no. 3, pp. 2333–2345, Mar. 2022.
[13] W. Mei and R. Zhang, "Performance analysis and user association optimization for wireless network aided by multiple intelligent reflecting surface," *IEEE Trans. Commun.*, vol. 69, no. 9, pp. 6296–6312, Sep. 2021.
[14] L. Yang *et al.*, "Secrecy performance analysis of RIS-aided wireless communication systems," *IEEE Trans. Veh. Technol.*, vol. 69, no. 10, pp. 12296–12300, Oct. 2020.
[15] X. Pang *et al.*, "IRS-assisted secure UAV transmission via joint trajectory and beamforming design," *IEEE Trans. Commun.*, vol. 70, no. 2, pp. 1140–1152, Feb. 2022.
[16] S. Fang, G. Chen, and Y. Li, "Joint optimization for secure intelligent reflecting surface assisted UAV networks," *IEEE Commun. Lett.*, vol. 10, no. 2, pp. 276–280, May 2021.
[17] X. Pang *et al.*, "When UAV meets IRS: Expanding air-ground networks via passive reflection," *IEEE Wireless Commun.*, vol. 28, no. 5, pp. 164–170, Oct. 2021.
[18] F. Shu *et al.*, "Enhanced secrecy rate maximization for directional modulation networks via IRS," *IEEE Trans. Commun.*, vol. 69, no. 12, pp. 8388–8401, Dec. 2021.
[19] B. Di *et al.*, "Hybrid beamforming for reconfigurable intelligent surface based multi-user communications: Achievable rates with limited discrete phase shifts," *IEEE J. Sel. Areas Commun.*, vol. 38, no. 8, pp. 1809–1822, Aug. 2020.
[20] J. Choi, G. Kwon, and H. Park, "Multiple intelligent reflecting surfaces for capacity maximization in LOS MIMO systems," *IEEE Wireless Commun. Lett.*, vol. 10, no. 8, pp. 1727–1731, Aug. 2021.
[21] H. U. Rehman, F. Bellili, A. Mezghani, and E. Hossain, "Joint active and passive beamforming design for IRS-assisted multi-user MIMO systems: A VAMP-based approach," *IEEE Trans. Commun.*, vol. 69, no. 10, pp. 6734–6749, Oct. 2021.
[22] Y. Han, S. Zhang, L. Duan, and R. Zhang, "Double-IRS aided MIMO communication under LoS channel: Capacity maximization and scaling," *IEEE Trans. Wireless Commun.*, vol. 70, no. 4, pp. 1–1, Apr. 2022.
[23] H.-M. Wang, J. Bai, and D. Limeng, "Intelligent reflecting surfaces assisted secure transmission without eavesdropper's csi," *IEEE Signal Process. Lett.*, vol. 27, pp. 1300–1304, Jul. 2020.
[24] Q. Wu and R. Zhang, "Beamforming optimization for intelligent reflecting surface with discrete phase shifts," *Proc. IEEE ICASSP*, pp. 7830–7833, May 2019.
[25] W. Shi, J. Li, G. Xia, Y. Wang, X. Zhou, Y. Zhang, and F. Shu, "Secure multigroup multicast communication systems via intelligent reflecting surface," *China Communications*, vol. 18, no. 3, pp. 39–51, Mar. 2021.
[26] Y. Zhang, C. Zhong, Z. Zhang, and W. Lu, "Sum rate optimization for two way communications with intelligent reflecting surface," *IEEE Commun. Lett.*, vol. 24, no. 5, pp. 1090–1094, May 2020.
[27] H. Shen, T. Ding, W. Xu, and C. Zhao, "Beamforming design with fast convergence for IRS-aided full-duplex communication," *IEEE Commun. Lett.*, vol. 24, no. 12, pp. 2849–2853, Dec. 2020.
[28] L. Yang, Y. Yang, M. O. Hasna, and M.-S. Alouini, "Coverage, probability of SNR gain, and DOR analysis of RIS-aided communication systems," *IEEE Wireless Commun. Lett.*, vol. 9, no. 8, pp. 1268–1272, Aug. 2020.
[29] C. Pan *et al.*, "Multicell MIMO communications relying on intelligent reflecting surfaces," *IEEE Trans. Wireless Commun.*, vol. 19, no. 8, pp. 5218–5233, Aug. 2020.
[30] J. Li *et al.*, "Performance analysis of directional modulation with finite-quantized RF phase shifters in analog beamforming structure," *IEEE Access*, vol. 7, pp. 97 457–97 465, Jul.. 2019.
[31] Z. Wei, C. Masouros, and F. Liu, "Secure directional modulation with few-bit phase shifters: optimal and iterative-closed-form designs," *IEEE Trans. Commun.*, vol. 69, no. 1, pp. 486–500, Jan. 2021.
[32] R. Dong, B. Shi, X. Zhan, F. Shu, and J. Wang, "Performance analysis of massive hybrid directional modulation with mixed phase shifters," *IEEE Trans. Veh. Technol.*, vol. 71, no. 5, pp. 5604–5608, May 2022.
[33] C. You, B. Zheng, and R. Zhang, "Channel estimation and passive beamforming for intelligent reflecting surface: Discrete phase shift and progressive refinement," *IEEE J. Sel. Areas Commun.*, vol. 38, no. 11, pp. 2604–2620, Nov. 2020.
[34] L. Wasserman, "All of statistics: A concise course in statistical inference," *New York, NY, USA: Springer*, 2004.
[35] T. K. Moon and W. C. Stirling, "Mathematical methods and algorithms for signal processing," *USA: Marsha Horron*, 1999.

Rongen Dong is currently pursuing the Ph.D. degree with the School of Information and Communication Engineer, Hainan University, China. Her research interests include physical layer security and directional modulation networks.

Yin Teng received the B.S. degree from ZiJin College at Nanjing University of Science and Technology, China, in 2019. She is currently working towards the M. S degree in the School of Electronic and Optical Engineering, Nanjing University of Science and Technology, Nanjing, China. Her research interests include wireless communication and signal processing.

Zhongwen Sun received the B.S. degree from Nanjing University of Science and Technology, Nanjing, China, in 2017. He is currently pursuing the M.S. degree with the School of Information and Communication Engineering, Hainan University, Haikou, China. His research interests include wireless communication and channel estimation for IRS-aided networks.

Jun Zou received the B.Eng. and Ph.D. degrees in Communication and Information System from Nanjing University of Science and Technology in 2011 and 2016, respectively. He is currently an Associate Professor with the School of Electronic and Optical Engineering, Nanjing University of Science and Technology. In 2019, he was a Research Associate with the Department of Electrical Engineering, City University of Hong Kong. His research interests are in the areas of wireless communications, signal processing and Internet of Things.

Mengxing Huang is currently a Professor and PhD Supervisor of Information Science and Technology, and the Dean of School of Information and Communication Engineering. His current research interests include big data and intelligent information processing, multi-source information collaborative perception and fusion, AI and smart services, etc., and he has published more than 200 academic papers as the first or corresponding author, 150 of these indexed by the SCI or EI. He owns 16 patents of invention, and 92 software copyright, and published 2 monographs and 2 translations. In recent years, he has undetaken more than 20 national or provicial projects. He has been awarded 1 First Class and 2 Second Class Prizes of The Hainan Provincial Scientific and Technological Progress. He is a member of IEEE, and a Senior Member of Chinese Computer Federation (CCF).

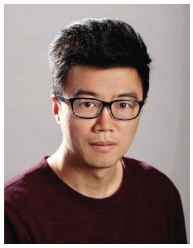

Jun Li (M'09-SM'16) received the Ph.D. degree in electronic engineering from Shanghai Jiao Tong University, Shanghai, China, in 2009. From January 2009 to June 2009, he was with the Department of Research and Innovation, Alcatel Lucent Shanghai Bell, as a Research Scientist. Since 2015, he is with the School of Electronic and Optical Engineering, Nanjing University of Science and Technology, Nanjing, China. His research interests include network information theory, channel coding theory, wireless network coding, and cooperative communications.

Feng Shu was born in 1973. He received the Ph.D., M.S., and B.S. degrees from the Southeast University, Nanjing, in 2002, XiDian University, Xian, China, in 1997, and Fuyang teaching College, Fuyang, China, in 1994, respectively. From Sept. 2009 to Sept. 2010, he is a visiting post-doctor at the University of Texas at Dallas. From Oct. 2005 to Nov. 2020, he was with the School of Electronic and Optical Engineering, Nanjing University of Science and Technology, Nanjing, China. Since Dec. 2020, he has been with the School of Information and Communication Engineering, Hainan University, Haikou, where he is currently a Professor and Supervisor of Ph.D and graduate students. He is awarded with Leading-talent Plan of Hainan Province, Mingjian Scholar Chair Professor and Fujian hundred-talent plan in Fujian Province. His research interests include wireless networks, wireless location, and array signal processing. Now, he is an Editor for the journals IEEE Wireless Communications Letters and IEEE Systems Journal. He has published more than 300 in archival journals with more than 100 papers on IEEE Journals and 160 SCI-indexed papers. He holds sixteen Chinese patents. Email: shufeng0101@163.com.

Jiangzhou Wang (Fellow, IEEE) has been a Professor since 2005 at the University of Kent, U.K. He has published over 400 papers and 4 books in the areas of wireless communications. Professor Wang is a Fellow of the Royal Academy of Engineering, U.K., Fellow of the IEEE, and Fellow of the IET. He was a recipient of the Best Paper Award from the IEEE GLOBECOM2012. He was an IEEE Distinguished Lecturer from 2013 to 2014. He was the Technical Program Chair of the 2019 IEEE International Conference on Communications (ICC2019), Shanghai, the Executive Chair of the IEEE ICC2015, London, and the Technical Program Chair of the IEEE WCNC2013. He has served as an Editor for a number of international journals, including IEEE Transactions on Communications from 1998 to 2013.